



PERGAMON

International Journal of Multiphase Flow 28 (2002) 1929–1944

International Journal of
**Multiphase
Flow**

www.elsevier.com/locate/ijmulflow

On the onset of flow instabilities in granular media due to porosity inhomogeneities

Theo Wilhelm ^{a,*}, Krzysztof Wilmański ^b

^a *Inst. für Geotechnik und Tunnelbau, Universität Innsbruck, Technikerstrasse 13, A-6020 Innsbruck, Austria*

^b *Weierstrass Institute, D-10117 Berlin, Germany*

Received 23 January 2001; accepted 1 September 2002

Abstract

The paper concerns a theoretical description able to capture the onset of instabilities in saturated sands at high filtration velocities (e.g. the onset of piping phenomena). Motivated by own experiments we propose a thermodynamical two component model which accounts for a threshold effect at a critical value of the relative velocity of components. This property is incorporated in the source term of momentum balance equations by means of a nonlinear contribution accounting for spatial variations of the porosity. We prove the thermodynamical admissibility of such a model. By means of a linear stability analysis we show the existence of the onset of instability for realistic values of material parameters gained from experiments.

© 2002 Elsevier Science Ltd. All rights reserved.

Keywords: Piping; Channeling; Flow instability in granular materials; Multicomponent model of saturated soils

1. Introduction

We aim to construct a macroscopic model of water flows through sandy soils able to capture the point of loss of stability related to rapid changes of permeability. These changes are due to inhomogeneities of porosity which influence momentum exchange between components. In experiments one observes these phenomena in form of channels appearing in an initially homogeneous material. This leads, in turn, to local increments of flow velocities, fluidization and erosion take place destroying locally parts of the soil skeleton. Details concerning the physical motivation,

* Corresponding author. Tel.: +43-676-666-2805; fax: +43-512-902-2850.
E-mail address: theo.wilhelm@uibk.ac.at (T. Wilhelm).



Fig. 1. Piping failure at Baldwin Hills Reservoir, California 1963 (Cedergren, 1967).

experimental evidence, and geophysical relevance can be found in the Ph.D. Thesis of Theo Wilhelm (Wilhelm, 2000).

Such channeling processes in saturated granular media are of interest in various fields of application. Their consequences in geotechnical engineering are frequently disastrous. As an illustrative example the effect of piping on the “Baldwin Hills” reservoir is shown in Fig. 1.

Inspection of seepage experiments which we describe in the next section, and in which water flows through a macroscopically homogeneous ¹ grain skeleton of sand, reveals the following characteristic phenomena:

- (i) At fluid velocities small compared to the minimum fluidizing velocity ² the macroscopic homogeneity is preserved. Porosity, permeability, and thus fluid flow rates remain constant throughout the system.
- (ii) When the fluid velocity further increases macroscopic inhomogeneities in form of channels directed towards the flow direction begin to form. Flows in smaller channels are attracted by bigger ones.
- (iii) When a big channel reaches the surface of the sample the flow behavior changes significantly. The flow rate increases rapidly and it is concentrated mainly within the big channel. Smaller channels form back or change their directions towards the main channel.

¹ The terms *microscopic* and *macroscopic* are used in a continuum mechanical sense (e.g. Bear, 1972).

² The minimum fluidizing velocity is the velocity at which the Terzaghi effective stress theoretically vanishes and the grain skeleton (theoretically) loses its strength. The hydraulic gradient is equal to the critical hydraulic gradient (see Wilhelm (2000) for further details and references).

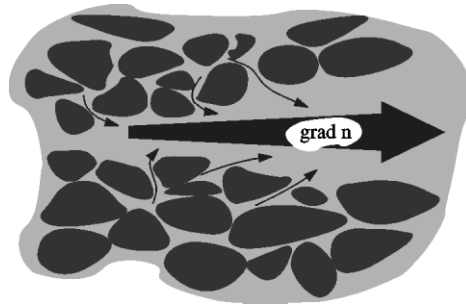


Fig. 2. Flow in a conically shaped pore channel (schematic).

These observations suggest that the fluid/grain skeleton interactions are sensitive to spatial variations of the porosity.

According to the above described observations we have to construct a model which yields an instability of flows appearing for sufficiently high porosity gradients, and sufficiently high relative velocities. We construct such a model by a modification of the momentum source appearing in two component models of saturated granular materials. In terms of models based on a Darcy law it means that we are modifying the Darcy law by making it dependent on the porosity gradient with a threshold behavior with respect to the relative velocity. It is demonstrated in Fig. 2: The flow resistance in a conically formed pipe or pore channel is smaller towards the direction of the widening of the channel.

Such a model must be necessarily nonlinear in its dependence on the relative velocity but not on the porosity gradient. We incorporate these requirements through a modification of the momentum source in the two component model. This requires a verification of thermodynamical conditions imposed on the model by the second law of thermodynamics. For this reason we devote Section 3, and the appendix of this paper to the evaluation of thermodynamical admissibility conditions.

We limit the attention to small elastic deformations of the skeleton. This limitation is not very crucial for the stability analysis shown in Section 4, as it is performed by means of a linear perturbation method which is not influenced by mechanical nonlinearities within the stress tensor of the skeleton. We also assume the isotropy of the system, and neglect viscous effects in the partial stresses of the fluid component. All these assumptions are made in order to expose better the main property of the model yielding the instability of flows and piping effects. Incidentally the lack of macroscopic viscosity of the fluid component does not mean that the real fluid is inviscid. It is known that some of those microscopic viscous properties are hidden in momentum sources of the macroscopic model.

In Section 4 we present the main results of the work. We investigate the stability of homogeneous seepage processes by superposing a small dynamical perturbation. We show that the dispersion relation may indeed contain solutions leading to the instability provided a material coefficient Γ which describes an influence of the porosity gradient on the exchange of momentum between components is sufficiently large. This result is illustrated by an example in the last section of the paper.

2. Experiments

The stability of a (quartz) sand–water mixture at a critical upward fluid flow was investigated experimentally (Wilhelm, 2000). A 20 cm high column of fine quartz sand contained in a perspex cylinder was used as specimen (see Fig. 3a).

The pore water pressure at the bottom of the column (2) was controlled by changes of the level of container (1) and the outflux at the top of the column was measured (3). The permeability and the relative fluid velocity were calculated from the geometry of the specimen, the applied pressure gradient and the water outflux. Fig. 3b shows the filter velocity, $v_f := nv^F$, as a function of the applied pressure gradient in terms of the hydraulic gradient, $i := \partial_z p / (\rho^F g) - 1$ (the signs are due to the conventions that p is positive for compression, and gravitation g is pointing towards the positive z -direction). At the rapid fluid velocity increment shown in Fig. 3b a channel has formed. The system has lost stability.

This loss of stability is related to the formation of a structure demonstrated in Fig. 4.

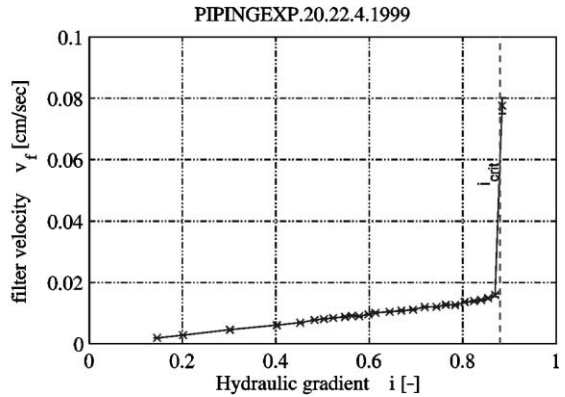
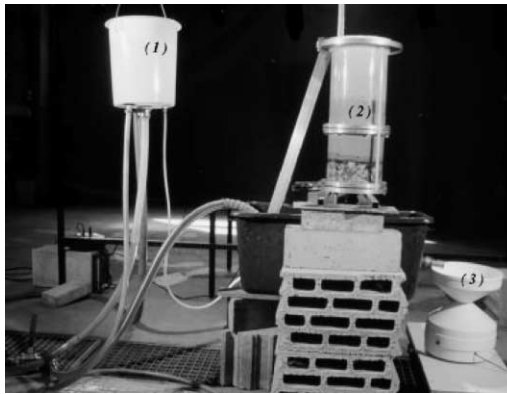


Fig. 3. (a) Setup of seepage experiments (left): (1) indicates the water source; (2) the specimen and (3) the output flux measuring unit. (b) Result of a seepage experiment with a quartz sand–water mixture (right): the course of the filter velocity nv^F against the applied pore water pressure gradient in terms of the hydraulic gradient $i := \partial_z p^F / (\rho^F g) - 1$ is shown.

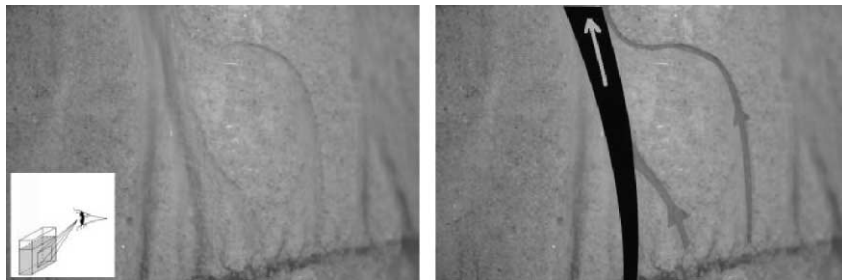


Fig. 4. Pipe formation in seepage experiment. Picture from a seepage experiment: At high fluid velocities channels start to select a big channel (marked as a dark shadow on the right) for the flow in the direction to the top, while small channels are reoriented in direction of the big channel (light shadows on the right). The small picture in the box indicates the position of the camera, and the area of the experimental glass container (size $42 \times 13 \times 56$ cm) reproduced in pictures.

The sample transforms from a homogeneous state not shown in this figure to a configuration with a pattern of several small channels dominated by a big channel (Fig. 4).

3. Construction of a macroscopical model

3.1. Fields and basic assumptions

We rely on a macroscopic two component description of saturated granular materials. Then in a continuum mechanical model processes are described by the following fields:

$$(\mathbf{x}, t) \mapsto \{\rho^S, \rho^F, n, u_k^S, v_k^F\}, \quad k = 1, 2, 3, \quad (1)$$

where \mathbf{x} denotes a current position of a particle of a solid component simultaneously occupied by a particle of the fluid component (continuous mixture), t is an instant of time and the fields are denoted as follows. ρ^S, ρ^F are the current partial mass densities of the solid and fluid component, respectively, $n \in [0, 1]$ is the porosity (the volume fraction of the fluid component related to the total representative volume element, *REV*), u_k^S —the displacement of the solid, v_k^F —the velocity of the fluid. We use Cartesian coordinates $\{x^k\}_{k=1,2,3}$.

According to these definitions the quantity

$$w_k := v_k^F - v_k^S, \quad v_k^S := \frac{\partial u_k^S}{\partial t} \quad (2)$$

describes the relative (seepage) velocity (e.g. Kolymbas, 1998, p. 26).

As we aim to describe solely certain stability properties of flows in such materials we neglect the compressibility of real materials. This yields some thermodynamical limitations as well as limitations of modes of propagation of waves. The former will be investigated in the sequel, the latter are immaterial for our present purposes. Consequently we make the following assumption:

$$\rho^S = (1 - n)\rho^{SR}, \quad \rho^{SR} = \text{const.}, \quad \rho^F = n\rho^{FR}, \quad \rho^{FR} = \text{const.}, \quad (3)$$

where ρ^{FR}, ρ^{SR} are the so called “real” mass densities of components.

This assumption reduces the set of fields (1) to the fields of porosity n , displacement u_k^S , and velocity v_k^F .

We require that field equations should follow from balance laws of mass and momentum for both components supplemented with appropriate constitutive relations. We limit attention to isotropic poroelastic materials and ideal fluids. We explain the physical contents of these assumptions in the next section.

It is obvious from the choice of fields that we consider solely isothermal processes, i.e. temperature will not appear anywhere in this model in the explicit form.

3.2. Field equations

As mentioned above we rely on partial balance equations for the two component system. Under the incompressibility assumption described in the previous section the mass balance equations reduce to the following form (e.g. Wilmański, 2001):

$$\frac{\partial n}{\partial t} + \frac{\partial}{\partial x^k} (nv_k^F) = 0, \quad \frac{\partial}{\partial x^k} [(1 - n)v_k^S + nv_k^F] = 0. \tag{4}$$

On the other hand the partial momentum equations are as follows:

$$\begin{aligned} \rho^S \left(\frac{\partial v_k^S}{\partial t} + v_l^S \frac{\partial v_k^S}{\partial x^l} \right) &= \frac{\partial T_{kl}^S}{\partial x^l} + p_k^*, \\ \rho^F \left(\frac{\partial v_k^F}{\partial t} + v_l^F \frac{\partial v_k^F}{\partial x^l} \right) &= \frac{\partial T_{kl}^F}{\partial x^l} - p_k^*, \end{aligned} \tag{5}$$

where we use the following notation: T_{kl}^F, T_{kl}^S —the partial Cauchy stress tensors, p_k^* —the momentum source (diffusion force, internal friction, etc.), v_k^F, v_k^S —the partial velocities. We have neglected body forces for simplicity. They do not influence thermodynamical considerations which we present in the next section, and they can be easily supplemented when needed in applications.

These equations become field equations if we specify constitutive relations. For the purpose of this work we choose the following set of constitutive variables

$$\mathfrak{B} := \left\{ n, \frac{\partial n}{\partial x^k}, e_{kl}, w_k \right\}, \tag{6}$$

where

$$\begin{aligned} e_{kl} &:= \frac{1}{2} \left(\frac{\partial u_k^S}{\partial x^l} + \frac{\partial u_l^S}{\partial x^k} \right) \equiv \frac{\partial u_k^S}{\partial x^l}, \\ \|e_{kl}\| &\equiv \max(|\lambda_e^1|, |\lambda_e^2|, |\lambda_e^3|) \ll 1 \end{aligned} \tag{7}$$

denote the deformation tensor of the solid component (skeleton). The deformation of the skeleton is assumed to be small, i.e. the biggest absolute value of the eigenvalues λ_e of e_{kl} is much smaller than unity.

The above choice of constitutive variables justifies the names of components mentioned in Section 3.1. In the limit case $n = 0$ we deal with a linear elastic material, and in the limit case $n = 1$ we deal with an ideal (incompressible) fluid.

The following constitutive quantities must be specified:

$$\mathfrak{C} := \{T_{kl}^F, T_{kl}^S, p_k^*, \psi^F, \psi^S\}, \tag{8}$$

where ψ^F, ψ^S are the partial Helmholtz free energies. They are introduced below for thermodynamical reasons.

For these quantities we assume that the following constitutive relation holds:

$$\mathfrak{C} = \mathfrak{C}(\mathfrak{B}). \tag{9}$$

It is assumed to be sufficiently smooth.

Substitution of constitutive relations in the balance equations yields field equations of the model.

Let us mention that the number of field equations (two scalar equations following from mass balance, and two vector equations following from momentum balance, i.e. 8 equations) is higher than the number of fields (one scalar field of porosity n , and six components of two vector fields—

displacement of the skeleton u_k^S , and velocity of the fluid v_k^F , i.e. 7 fields). This is natural in the case of constraints, and an additional field must be introduced as a reaction force on the constraint. In our case it is the scalar field of pore water pressure p whose existence is motivated by the second law of thermodynamics as explained in Appendix A. In this way the model becomes consistent mathematically.

3.3. Thermodynamical admissibility of constitutive relations

It is customary to require in continuous models that a second law of thermodynamics satisfied by all solutions of field equations. For the class of isothermal processes considered in this work we assume this law to have the following form (e.g. Wilmanski, 2001). The inequality

$$\rho^S \left(\frac{\partial \psi^S}{\partial t} + v_k^S \frac{\partial \psi^S}{\partial x^k} \right) = \rho^F \left(\frac{\partial \psi^F}{\partial t} + v_k^F \frac{\partial \psi^F}{\partial x^k} \right) - T_{kl}^S \frac{\partial v_k^S}{\partial x^l} - T_{kl}^F \frac{\partial v_k^F}{\partial x^l} - p_k^* w_k \leq 0 \quad (10)$$

must be identically satisfied for all solutions of field equations.

The second law is usually formulated as an entropy inequality. It reduces to the above form under the assumption of constant temperature. The Helmholtz free energies ψ^S, ψ^F are introduced for convenience. If $\varepsilon^S, \varepsilon^F$ denote the densities of partial internal energies and η^S, η^F —the densities of partial entropies then

$$\psi^S := \varepsilon^S - T\eta^S, \quad \psi^F := \varepsilon^F - T\eta^F. \quad (11)$$

A rather technical evaluation of the inequality (10) is presented in Appendix A. We proceed to specify constitutive relations for partial stresses T_{kl}^F, T_{kl}^S , and for the momentum source satisfying the above inequality.

Let us begin with the momentum source. According to the thermodynamic considerations presented in Appendix A it has the following structure:

$$p_k^* = \Pi w_k - \left(p + \rho^S \frac{\partial \psi^S}{\partial n} \right) \frac{\partial n}{\partial x^k}. \quad (12)$$

The coefficient Π is the material parameter describing the permeability of the skeleton. It depends on the porosity n . However this dependence is immaterial for the analysis of this work because it appears in the product with the relative velocity w_k . Consequently it is nonlinear, and such contributions do not influence the linear stability analysis presented further in this work. However, it should be born in mind that the coefficient Π still depends parametrically on an initial porosity.

Unspecified remains the contribution of the free energy. We relate this part to the threshold effects appearing at the beginning of piping. Namely we assume that it has the following form:

$$\rho^S \frac{\partial \psi^S}{\partial n} = -\rho^F \frac{\partial \psi^F}{\partial n} = \frac{\Gamma}{\sqrt{2}} \left(1 + \frac{W - Y}{|W - Y|} \right) \sqrt{W}, \quad \Gamma, Y > 0, \quad W := \frac{1}{2} w_k w_k, \quad (13)$$

where the material parameter Γ may be still dependent on the porosity n , deformation of the skeleton e_{kl} , and the invariant of the relative velocity W . The expression in parenthesis introduces the threshold behavior into the model. Its existence has been indicated in Section 2 (see Fig. 3b).

The constant $\sqrt{2Y}$ denotes the threshold. As we see further it yields flow instabilities for relative velocities whose magnitude exceeds the limit $\sqrt{2Y}$. It needs to be determined experimentally, however, in a first approximation it can be set equal to the minimum fluidizing velocity. This relation is motivated by thermodynamic identities for free energy functions presented in Appendix A, and in particular by the results for the dependence of free energies on the porosity in the static case (A.15)₂. A physically motivated, less elaborate deduction is given in (Wilhelm, 2000, p. 52).

For the partial stress tensors T_{kl}^S , T_{kl}^F we assume in addition that they do not contain contributions of the relative velocity w_k . Otherwise we would have some sort of viscid reactions of the material which we excluded from the beginning of the construction of the model. Inspection of relations (A.7) and (A.8) shows that such contributions would be of the order higher than one in w_k . Such an assumption together with (13) yields the following constitutive relations:

$$\begin{aligned} T_{kl}^S &= -(1-n)p\delta_{kl} + \frac{\partial}{\partial e_{kl}}(\rho^S\psi^S + \rho^F\psi^F), \\ T_{kl}^F &= -np\delta_{kl}. \end{aligned} \quad (14)$$

In addition the assumption on small deformations of the isotropic skeleton yields Hooke's relation in the partial stress T_{kl}^S

$$\frac{\partial}{\partial e_{kl}}(\rho^S\psi^S + \rho^F\psi^F) = \lambda^S e_{mm}\delta_{kl} + 2\mu^S e_{kl}, \quad (15)$$

where λ^S , μ^S are Lamé parameters dependent solely on the porosity n .

The momentum balance equations (4) have then the following form:

$$\begin{aligned} \rho^S \left(\frac{\partial v_k^S}{\partial t} + v_l^S \frac{\partial v_k^S}{\partial x^l} \right) &= -(1-n) \frac{\partial p}{\partial x^k} + \frac{\partial}{\partial x^l} (\lambda^S e_{mm} \delta_{kl} + 2\mu^S e_{kl}) \\ &\quad + \Pi w_k - \frac{\Gamma}{\sqrt{2}} \left(1 + \frac{W-Y}{|W-Y|} \right) \sqrt{W} \frac{\partial n}{\partial x^k}, \\ \rho^F \left(\frac{\partial v_k^F}{\partial t} + v_l^F \frac{\partial v_k^F}{\partial x^l} \right) &= -n \frac{\partial p}{\partial x^k} - \Pi w_k + \frac{\Gamma}{\sqrt{2}} \left(1 + \frac{W-Y}{|W-Y|} \right) \sqrt{W} \frac{\partial n}{\partial x^k}, \quad \lambda^S, \mu^S, \Pi, \Gamma, Y > 0. \end{aligned} \quad (16)$$

In the remaining part of this work we investigate linear stability properties of processes described by these equations.

Relations (13) and (15) yield integrability relations

$$\frac{\partial}{\partial e_{kl}} \left(\frac{\rho^F \psi^F}{n} - \frac{\rho^S \psi^S}{1-n} \right) = \frac{\partial}{\partial n} (\lambda^S e_{mm} \delta_{kl} + 2\mu^S e_{kl}), \quad (17)$$

which impose limitations of the dependence of material parameters λ^S , μ^S on the porosity n . For instance, if we assume that ψ^F is independent of e_{kl} we obtain a linear dependence on the porosity. As obtained from dynamical measurements (speeds of bulk waves in saturated granular materials) this is a relatively good approximation for porosities between, say, 0.05 to 0.6. Otherwise we have to construct a model without, for instance, the requirement (13). Simultaneously the definition of Γ which is a part of relation (13) has consequences on the behavior of material parameters λ^S , μ^S .

The above integrability conditions indicate that these parameters may change in a discontinuous manner at $W = Y$, i.e. by flows locally yielding fluidization. This is in accord with the remarks which we made in Section 1. We shall account for this property in the next section assuming that the elastic parameters become much smaller after fluidization.

4. Stability analysis

In this section a perturbation analysis for a saturated elastic grain skeleton subject to an upward fluid flow is shown. The nonlinear interaction term introduced in the previous section is taken into account. It is shown that the analysis is therefore capable to model the onset of experimentally observed instabilities that classical models are not able to describe.

4.1. Model

The calculation is based on the balance equations (3) and (16). Modelled is the vertical flow of water through a grain skeleton in a wide tube. Due to the boundary conditions (horizontal displacements are zero) the problem reduces to one dimension. Gravitation is considered in the calculation by adding appropriate body forces to the momentum balance equations, $\rho^S g$ in (16)₁ and $\rho^F g$ in (16)₂. It is assumed that the relative velocity has exceeded the threshold, $W > Y$, such that the nonlinear interaction term becomes active. In the one dimensional case only the components T_{33}^F , T_{33}^S and e_{33} appear in the calculation (not quoted here). Thus the indices will be skipped (e.g. $e := e_{33}$).

4.2. Field equations

Together with the compatibility condition relating the motion of the skeleton to the deformation:

$$\partial_t e = \partial_z v^S, \quad (18)$$

the equations for the fields $\{n, p, v^F, v^S, e\}$ are

$$\begin{aligned} \partial_t n + \partial_z [n v^F] &= 0, \\ -\partial_t n + \partial_z [(1-n)v^S] &= 0, \\ n \rho^{FR} [\partial_t v^F + v^F \partial_z v^F] &= -n \partial_z p + n \rho^{FR} g - \Pi(v^F - v^S) + \Gamma |v^F - v^S| \partial_z n, \\ (1-n) \rho^{SR} [\partial_t v^S + v^S \partial_z v^S] &= E \partial_z e - (1-n) \partial_z p + (1-n) \rho^{SR} g + \Pi(v^F - v^S) - \Gamma |v^F - v^S| \partial_z n, \\ \partial_t e &= \partial_z v^S. \end{aligned} \quad (19)$$

The elasticity parameter E of the grain skeleton is related to the Lamé parameters of the formula (15) by the classical relation $E = \lambda^S + 2\mu^S$. It is assumed to be constant in this linear analysis.

4.3. Ground state—homogeneous seepage

The stability of the uniform state of a granulate subject to an upward fluid flow is investigated. This state of uniform flow, indicated by the subscript 0, is characterized by

$$\begin{aligned}
 n(z, t) &= n_0 = \text{const}, \\
 v^S(z, t) &= v_0^S = 0, \\
 v^F(z, t) &= v_0^F = \text{const}, \\
 p(z, t) &= p_0(z), \\
 e(z, t) &= e_0 = -\frac{c_1}{E}z.
 \end{aligned} \tag{20}$$

The stress distribution in the grain skeleton follows to be a linear function of depth. From this and the constitutive relation for the skeleton, the deformation field for the ground state (20)₅ follows. The constant c_1 is positive, as stresses in the skeleton are defined negative for compression.

Substituting (20)_{1–5} into the field equations reduces them to the equations governing the equilibrium:

$$\begin{aligned}
 0 &= 0, \\
 0 &= 0, \\
 -\partial_z p_0 + \rho^{\text{FR}}g - \frac{\Pi}{n_0}v_0^F &= 0, \\
 -\frac{c_1}{1-n_0} - \partial_z p_0 + \rho^{\text{SR}}g + \frac{\Pi}{1-n_0}v_0^F &= 0, \\
 0 &= 0.
 \end{aligned} \tag{21}$$

These equations describe a steady ground state. In the case of a velocity controlled system³ the pore water pressure $p_0(z)$ and the deformation $e_0(z)$ can be calculated from these equations for a given fluid velocity v_0^F . In the case of a pressure gradient controlled system⁴ the fluid velocity v_0^F and the deformation $e_0(z)$ can be calculated for a given pressure gradient.

If c_1 is set equal to the submerged unit weight of the skeleton, $\gamma'_0 := (1-n_0)(\rho^{\text{SR}} - \rho^{\text{FR}})_g$, Eq. (21)_{3–4} imply that v_0^F must vanish, thus describing the so called “geostatic” stress state consistently:

$$\begin{aligned}
 Ee_0 &= -\gamma'_0 z, \\
 p_0 &= \rho^{\text{FR}}gz.
 \end{aligned} \tag{22}$$

4.4. Linear equations governing small perturbations

To study the stability of the steady ground state the fields (20)_{1–5} are augmented by small perturbations follow as

³ The fluid flow v_0^F is controlled in the experiment. The known porosity depends on the material used and the way the experiment is prepared.

⁴ The pore fluid pressure gradient $\partial_z p_0$ is controlled in the experiment.

$$\begin{aligned}
 n(z, t) &= n_0 + n_1(z, t), \\
 v^S(z, t) &= v_1^S(z, t), \\
 v^F(z, t) &= v_0^F + v_1^F(z, t), \\
 p(z, t) &= p_0(z) + p_1(z, t), \\
 e(z, t) &= e_0(z) + e_1(z, t).
 \end{aligned}
 \tag{23}$$

Substituting (23)_{1–5} into the field equations (19)_{1–5}, linearizing and considering the relations for the equilibrium solutions, (21)_{3–4}, the linearized equations governing the perturbations follow as

$$\begin{aligned}
 \partial_t n_1 + n_0 \partial_z v_1^F + v_0^F \partial_z n_1 &= 0, \\
 -\partial_t n_1 + (1 - n_0) \partial_z v_1^S &= 0, \\
 n_0 \rho^{\text{FR}} \partial_t v_1^F &= -n_1 \partial_z p_0 - n_0 \partial_z p_1 + n_1 \rho^{\text{FR}} g - \Pi(v_1^F - v_1^S) + \Gamma |v_0^F| \partial_z n_1, \\
 (1 - n_0) \rho^{\text{SR}} \partial_t v_1^S &= E \partial_z e_1 - (1 - n_0) \partial_z p_1 + n_1 \partial_z p_0 - n_1 \rho^{\text{SR}} g + \Pi(v_1^F - v_1^S) - \Gamma |v_0^F| \partial_z n_1, \\
 \partial_t e_1 &= \partial_z v_1^S.
 \end{aligned}
 \tag{24}$$

4.5. Solutions in the form of plane waves

The perturbations are assumed to be in the form of plane waves:

$$\begin{aligned}
 n_1(z, t) &= N e^{(st+ikz)}, \\
 v_1^S(z, t) &= V^S e^{(st+ikz)}, \\
 v_1^F(z, t) &= V^F e^{(st+ikz)}, \\
 p_1(z, t) &= P e^{(st+ikz)}, \\
 e_1(z, t) &= B e^{(st+ikz)}.
 \end{aligned}
 \tag{25}$$

Here the amplitudes N, V^S, V^F, P, B are constant and k is the wave vector. It corresponds to the wavelength by $2\pi/|k|$. This form of solution is possible due to the linearity of relations (22) with respect to the depth variable z . The factor s is in general complex, $s = a - ib$. The propagation velocity of the wave is $b/|k|$. The real part a determines the stability of the system. If it is negative or zero disturbances decay exponentially or remain small. The system is stable. If it is positive small disturbances grow exponentially with time.

Substituting the plane wave solutions (25)_{1–5} into the governing equations for the small perturbations, (24)_{1–5}, these degenerate into five linear equations for the five unknowns $x_k := (n_1, v_1^S, v_1^F, p_1, e_1)$:

$$A_{jk} x_k = 0$$

with

$$A_{jk} = \begin{pmatrix} s + v_0^F ik & 0 & n_0 ik & 0 & 0 \\ -s & (1 - n_0) ik & 0 & 0 & 0 \\ \partial_z p_0 - \rho^{\text{FR}} g - \Gamma |v_0^F| ik & -\Pi & n_0 \rho^{\text{FR}} s + \Pi & n_0 ik & 0 \\ -\partial_z p_0 + \rho^{\text{SR}} g + \Gamma |v_0^F| ik & (1 - n_0) \rho^{\text{SR}} s + \Pi & -\Pi & (1 - n_0) ik & -E ik \\ 0 & -ik & 0 & 0 & s \end{pmatrix}.$$

This system of linear equations has nontrivial solutions if and only if the determinant of its coefficient matrix A_{jk} vanishes. This condition leads to dispersion relation (third order polynomial) for s as a function of k . Its roots determine all possible plane wave modes for a given wave vector k . They were calculated using the algebra package MAPLE. As the expressions are rather lengthy they are not quoted here. Depending on the parameters gained from experiments the real part of s might be greater than zero for some wave vectors k . These modes lead to an exponential increase in the amplitude of the originally small perturbations and thus to an unstable behavior.

As parameters for the calculation values from the experiment presented in Fig. 3b close to its critical state were used:

$$\begin{aligned} \rho^{\text{SR}} &= 2650 \text{ kg/m}^3, \\ \rho^{\text{FR}} &= 1000 \text{ kg/m}^3, \\ n_0 &= 0.47, \\ \Pi &= n_0^2 \rho^{\text{FR}} g / \kappa = 1.2 \times 10^7 \text{ kg/(m}^3 \text{ s)}, \\ v_0^F &= -1.6 \times 10^{-4} \text{ m/s}, \\ \partial_z p_0 &= \rho^{\text{FR}} g - \frac{\Pi}{n_0} v_0^F = 14085 \text{ Pa/m}. \end{aligned}$$

Here κ is the (Darcy) permeability evaluated from the experiment. The bulk modulus was assumed to be very small $E = 1.0$ Pa. This assumption is motivated by a dependence of the stiffness of sand from the mean stress. In the range well below the threshold the skeleton behaves in a rather stiff manner with values of material parameters different from those in the vicinity of the point of fluidization. However the ground state belongs to this vicinity. There the sand loses its stiffness. This is the reason for the choice of the small value of E . Such a dependence was indicated at the end of Section 3.3.

Out of three roots Fig. 5 shows the significant root responsible for the unstable behavior.

The real part of s is plotted as a function of the wave number k and Γ , the parameter of the nonlinear interaction term. Regions where the real part of s is greater than zero represent unstable modes. It can be seen that there exist unstable modes for physically relevant parameters ($\Gamma > 0$, $E > 0$).

The onset of instability of the system could be modelled using even the simplest form of the nonlinear interaction term. The same calculation omitting the nonlinear interaction (by setting $\Gamma = 0$) does not show unstable modes ($\text{Re}(s) > 0$) unless the bulk modulus E is set to unrealistic, negative values (not quoted here).

The above results show that the new model can be used for more realistic conditions of flows in soils in order to describe the onset of unstable fluidization phenomena.

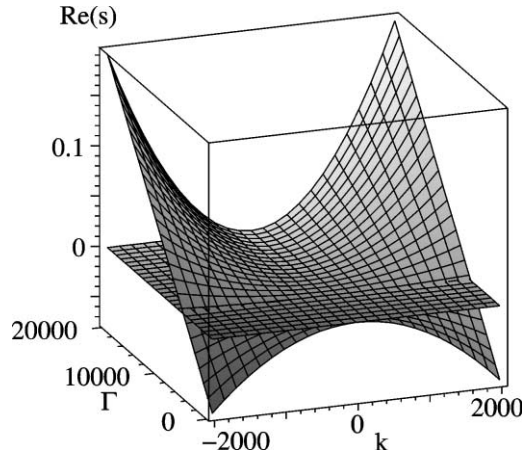


Fig. 5. Real part of one of the three roots of the dispersion relation as a function of the wave number k , and the material parameter appearing in the nonlinear interaction Γ . Unstable modes can be seen ($\text{Re}(s) > 0$) for $\Gamma \gtrsim 6000 \text{ kg}/(\text{m}^2 \text{ s})$. The bulk modulus used in the calculation is $E = 1.0 \text{ Pa}$.

Acknowledgement

This work was supported by the Austrian Science Fund (FWF) in the framework of the projects P10956-OETE and P12701-TEC.

Appendix A

It is customary to eliminate the restriction of the inequality (10) to solutions of field equations by means of Lagrange multipliers (e.g. Müller, 1985; Wilmanski, 1998). By doing so we obtain the following inequality which should hold for all fields, and not only for solutions of field equations

$$\begin{aligned} & \rho^S \left(\frac{\partial \psi^S}{\partial t} + v_k^S \frac{\partial \psi^S}{\partial x^k} \right) + \rho^F \left(\frac{\partial \psi^F}{\partial t} + v_k^F \frac{\partial \psi^F}{\partial x^k} \right) - T_{kl}^S \frac{\partial v_k^S}{\partial x^l} - T_{kl}^F \frac{\partial v_k^F}{\partial x^l} - p_k^* w_k - A \left(\frac{\partial n}{\partial t} + \frac{\partial}{\partial x^k} (n v_k^F) \right) \\ & - \lambda \left(\frac{\partial}{\partial x^k} [(1-n)v_k^S + n v_k^F] \right) - A_k^F \left\{ \rho^F \left(\frac{\partial v_k^F}{\partial t} + v_l^F \frac{\partial v_k^F}{\partial x^l} \right) - \frac{\partial T_{kl}^F}{\partial x^l} + p_k^* \right\} \\ & - A_k^S \left\{ \rho^S \left(\frac{\partial v_k^S}{\partial t} + v_l^S \frac{\partial v_k^S}{\partial x^l} \right) - \frac{\partial T_{kl}^S}{\partial x^l} - p_k^* \right\} \leq 0. \end{aligned} \tag{A.1}$$

Lagrange multipliers A, λ, A_k^F, A_k^S are functions of constitutive variables \mathfrak{B} .

After application of the chain rule of differentiation in the inequality (A.1) the linearity with respect to some derivatives can be seen. This yields the condition that coefficients of these derivatives must vanish identically. We obtain for the coefficients of time derivatives:

$$\frac{\partial n}{\partial t} : \quad A = \rho^S \frac{\partial \psi^S}{\partial n} + \rho^F \frac{\partial \psi^F}{\partial n}, \tag{A.2}$$

$$\frac{\partial}{\partial t} \frac{\partial n}{\partial x^k} : \frac{\partial}{\partial \frac{\partial n}{\partial x^k}} (\rho^S \psi^S + \rho^F \psi^F) = 0, \quad (\text{A.3})$$

$$\frac{\partial v^F}{\partial t} : \rho^F A_k^F = \frac{\partial}{\partial w_k} (\rho^S \psi^S + \rho^F \psi^F), \quad (\text{A.4})$$

$$\frac{\partial v^S}{\partial t} : \rho^S A_k^S = -\frac{\partial}{\partial w_k} (\rho^S \psi^S + \rho^F \psi^F). \quad (\text{A.5})$$

Consequently

$$\rho^F A_k^F = -\rho^S A_k^S. \quad (\text{A.6})$$

and, according to relation (A.3), multipliers A_k^F, A_k^S are independent of the gradient $\partial n / \partial x_k$.

On the other hand the coefficients of spatial derivatives lead to identities:⁵

$$\frac{\partial v_k^S}{\partial x^l} : T_{kl}^S = -(1-n)\lambda \delta_{kl} + \frac{\partial}{\partial e_{kl}} (\rho^S \psi^S + \rho^F \psi^F) - \rho^F \frac{\partial \psi^F}{\partial w_k} w_l - \frac{\partial T_{ml}^S}{\partial w_k} A_m^S - \frac{\partial T_{ml}^F}{\partial w_k} A_m^F, \quad (\text{A.7})$$

$$\frac{\partial v_k^F}{\partial x^l} : T_{kl}^F = -n\lambda \delta_{kl} - n \left(\rho^S \frac{\partial \psi^S}{\partial n} + \rho^F \frac{\partial \psi^F}{\partial n} \right) \delta_{kl} - \rho^S \frac{\partial \psi^S}{\partial w_k} w_l + \frac{\partial T_{ml}^S}{\partial w_k} A_m^S + \frac{\partial T_{ml}^F}{\partial w_k} A_m^F, \quad (\text{A.8})$$

$$\frac{\partial^2 n}{\partial x^k \partial x^l} : \frac{\partial}{\partial \frac{\partial n}{\partial x^k}} (\rho^S \psi^S w_l - A_m^S T_{l/m}^S - A_m^F T_{l/m}^F) = 0, \quad (\text{A.9})$$

where the condition (A.2) was applied.

The condition following from the linearity with respect to the derivative $\partial e_{kl} / \partial x^m$ is immaterial for further considerations, and we shall not quote it here.

It remains the following nonlinear part of the inequality which is called the residual inequality:

$$\left(\rho^S \frac{\partial \psi^S}{\partial n} + \lambda \right) w_k \frac{\partial n}{\partial x^k} + (w_k + A_k^F - A_k^S) p_k^* \geq 0. \quad (\text{A.10})$$

It defines the dissipation in processes.

Let us notice that the dissipation contains an explicit dependence on the Lagrange multiplier λ . This multiplier plays the role of the reaction force on the constraint following from the assumption on incompressibility of real components (compare Wilmański, 2001). Consequently it should be determined by field equations rather than by a constitutive relation, and it should not appear in the dissipation inequality as the constraint (3)₂ is holonomous (i.e. nondissipative). Hence the inequality (A.10) cannot contain linear contributions of the porosity gradient, and this yields the necessity of dependence of the momentum source on this gradient.

We do not investigate the above results in their full generality, and proceed to simplifications yielding a model sufficient for our purposes.

⁵ The time derivative $\partial e_{kl} / \partial t$ gives only a subclass of the conditions quoted below due to the relation

$$\frac{\partial e_{kl}}{\partial t} = \frac{1}{2} \left(\frac{\partial v_k^S}{\partial x^l} + \frac{\partial v_l^S}{\partial x^k} \right).$$

We assume the system to be isotropic, and linear with respect to a dependence on the porosity gradient $\partial n / \partial x^k$. This means that neither free energies ψ^S, ψ^F , nor partial stress tensors T_{kl}^S, T_{kl}^F , may depend on the porosity gradient. Then the identities (A.3) and (A.9) are identically satisfied. Simultaneously we have the following representation for the momentum source (an isotropic vector function of two vectorial constitutive variables)

$$p_k^* = \Pi w_k + v \frac{\partial n}{\partial x^k} + \theta \varepsilon_{klm} w_l \frac{\partial n}{\partial x^m}, \tag{A.11}$$

where Π, v, θ are scalar functions of invariants: $W := \frac{1}{2} w_k w_k$, and $w_k (\partial n / \partial x^k) \varepsilon_{klm}$ is the permutation symbol. Substitution in (A.10) yields

$$\begin{aligned} & \left[\lambda + v + \rho^S \frac{\partial \psi^S}{\partial n} + v \left(\frac{1}{\rho^F} + \frac{1}{\rho^S} \right) \frac{\partial}{\partial W} (\rho^S \psi^S + \rho^F \psi^F) \right] w_k \frac{\partial n}{\partial x^k} \\ & + \Pi \left[1 + \left(\frac{1}{\rho^F} + \frac{1}{\rho^S} \right) \frac{\partial}{\partial W} (\rho^S \psi^S + \rho^F \psi^F) \right] w_k w_k \geq 0. \end{aligned} \tag{A.12}$$

We have used here the identity (A.2), and, in addition, we left out the dependence on non-linear invariants containing contributions of e_{kl} . The latter simplification is due to the assumption (6).

Apparently the contribution with the coefficient θ does not appear in the dissipation inequality (A.12). It means its sign can be arbitrary as far as the thermodynamical admissibility is concerned. Simultaneously the loss of stability in piping processes is irreversible. It means that it cannot be related to the contribution with θ . Consequently we can assume in our stability analysis that $\theta = 0$. It should be stressed, however, that the role of this contribution in flow processes has not been sufficiently investigated as yet.

According to the previous remarks we have to choose v in such a way that the contribution of λ to (A.12) disappears. We proceed to investigate this problem.

The linearity with respect to the porosity gradient, and the assumption that λ is a field yield:

$$\lambda + v + \rho^S \frac{\partial \psi^S}{\partial n} = 0, \quad \frac{\partial}{\partial W} (\rho^S \psi^S + \rho^F \psi^F) = 0. \tag{A.13}$$

On the other hand in static processes ($v_k^F = 0, v_k^S = 0$) the momentum balance of the fluid (4)₂, and relation (A.8) yield:

$$-\frac{\partial p^F}{\partial x^k} - v \Big|_{w_k=0} \frac{\partial n}{\partial x^k} = 0, \quad p^F := n \left(\lambda + \left(\rho^S \frac{\partial \psi^S}{\partial n} + \rho^F \frac{\partial \psi^F}{\partial n} \right) \Big|_{w_k=0} \right). \tag{A.14}$$

Simultaneously we expect in this case that the pore water pressure p and the partial pressure in the fluid p^F are related to each other: $p^F = np$ (Bear, 1972). On the other hand the expression in parenthesis of (A.14)₂ cannot be constant in general as the free energies depend, for instance, on the deformation e_{kl} . Consequently, the above relation for the partial pressure, and the fact that the pore water pressure p is constant in such static experiments we must require:

$$p = -v \Big|_{w_k=0}, \quad \left(\rho^S \frac{\partial \psi^S}{\partial n} + \rho^F \frac{\partial \psi^F}{\partial n} \right) \Big|_{w_k=0} = 0, \quad \lambda = p. \tag{A.15}$$

It follows from (A.13)₁

$$\rho^S \frac{\partial \psi^S}{\partial n} \Big|_{w_k=0} = 0. \quad (\text{A.16})$$

Let us summarize the results. Relations (A.7) and (A.8) for partial stresses have the form

$$\begin{aligned} T_{kl}^S &= -(1-n)p\delta_{kl} + \frac{\partial}{\partial e_{kl}} (\rho^S \psi^S + \rho^F \psi^F) + \mathcal{O}(|w_k w_k|), \\ T_{kl}^F &= -np\delta_{kl} + \mathcal{O}(|w_k w_k|), \end{aligned} \quad (\text{A.17})$$

where the contributions $\mathcal{O}(|w_k w_k|)$ are nonlinear with respect to the relative velocity. Relation (A.11) reduces to the following one:

$$p_k^* = \Pi w_k - \left(p + \rho^S \frac{\partial \psi^S}{\partial n} \right) \frac{\partial n}{\partial x^k}, \quad (\text{A.18})$$

and the residual inequality (A.12) indicates solely the positiveness of the permeability coefficient Π .

References

- Bear, J., 1972. *Dynamics of Fluids in Porous Media*. Dover Publication, New York.
- Cedergren, H.R., 1967. *Drainage and Flow Nets*. John Wiley and Sons.
- Müller, I., 1985. *Thermodynamics*. Pitman, New York.
- Kolymbas, D., 1998. *Geotechnik—Bodenmechanik und Grundbau*. Springer, Berlin.
- Wilhelm, Th., 2000. *Piping in Saturated Granular Media*, Ph.D. Thesis, University of Innsbruck ftp://ftp.uibk.ac.at/pub/uni-innsbruck/igt/publications/_wilhelm/phd_thesis_wilhelm.pdf.
- Wilmanski, K., 2001. Note on the incompressibility in theories of porous and granular materials. *ZAMM* 81 (1), 37–42.
- Wilmanski, K., 1998. *Thermomechanics of Continua*. Springer, Berlin.